Chinese Chemical Letters 37 (2026) 111336

Contents lists available at ScienceDirect

Chinese Chemical Letters

journal homepage: www.elsevier.com/locate/cclet

Malbrumpenoids A-N, unusually cyclized triterpenoids from the *Euphorbia* endophyte *Malbranchea umbrina* D16

Shu-Qi Wu[a,1], Xinying Zhu[a,1], Fang-Yu Yuan[a], Han-Zhuang Weng[a,b], Lei Li[a], Dong Huang[a], Gui-Hua Tang[a,*], Sheng Yin[a,*]

[a] School of Pharmaceutical Sciences, Sun Yat-sen University, Guangzhou 510006, China
[b] State Key Laboratory of Ophthalmology, Zhongshan Ophthalmic Center, Sun Yat-sen University, Guangdong Provincial Key Laboratory of Ophthalmology Visual Science, Guangzhou 510060, China

ARTICLE INFO

Article history:
Received 25 February 2025
Revised 14 May 2025
Accepted 16 May 2025
Available online 16 May 2025

Keywords:
Endophytes
Malbranchea umbrina D16
Unusually cyclized triterpenoids
Malbrumpenoid
Antiadipogenic activity
AMP-activated protein kinase

ABSTRACT

Molecular networking-guided chemical investigation of the *Euphorbia* endophyte *Malbranchea umbrina* D16 led to the isolation of 14 novel unusually cyclized triterpenoids (UCT) involving three different skeletal types. Compounds **1**–**10** are tricyclic triterpenoids featuring a 1-cyclohexyloctahydro-1*H*-indene core, in which **1** incoporates an unusual 7,7-dimethyl-6,8-dioxabicyclo[3.1.2]octane motif. Compounds **11**–**13** represent a rare class of bicyclic triterpenes (6/5 ring system) containing various *O*-heterocycles at the side chain. Compound **14** is an acyclic triterpenoid with *O*-heterocycles at both ends. Their structures were assigned by spectroscopic, chemical, computational, and crystallographic means, which also allowed the stereochemical revisions of three previously reported analogues. Compound **1** significantly inhibited the adipogenesis in 3T3-L1 adipocytes *via* activating the AMP-activated protein kinase (AMPK) signalling.

© 2026 Published by Elsevier B.V. on behalf of Chinese Chemical Society and Institute of Materia Medica, Chinese Academy of Medical Sciences.

Triterpenoids represent one of the largest and most structurally diverse classes of natural products. Biogenetically, they are built up from six isoprene subunits *via* mevalonate pathway, utilizing the linear 30-carbon squalene (S) as the key precursor [1]. Further cyclization of S or its derivative 2,3-oxidosqualene (OS) in different manners contributes to diverse polycyclic skeletons of this class. Compared with the mainstream cascade cyclization, which typically generates tetra- or pentacyclic skeletons, the incomplete or two independent cyclizations of the linear precursors, as well as the ring cleavage lead to the biosynthesis of a rare group of mono-, bi- or tricyclic triterpenoids, collectively referred to as unusually cyclized triterpenoids (UCT) [2,3]. The intriguing structures of UCTs make them not only compelling synthetic targets, but also a promising arsenal for drug discovery. For instance, the monocyclic UCT marnerol, whose oxidation derivatives exhibited significant cytotoxicity, has been biosynthetically proved to derive from OS involving a Grob fragmentation process [4]. (−)-Abudinol B, a tricyclic UCT with a condensed oxepane-cycloalkane system, was biomimetically total synthesized by McDonald's group [5]. Yardenone 2, a bicyclic triterpene with 7/6/5–5/7 ring system, selectively inhibited the proliferation of hypoxic PC3 cells, suggesting a new avenue for prostate cancer therapy [6].

Endophytes are microorganisms inhabiting within the plants. Throughout an evolutionary process, these organisms have progressively developed intricate symbiotic relationships with plant hosts, among which mutualism interaction results in long-term coevolution between endophytes and host plants [7]. Such association confers genetic diversity on both partners and promotes the production of a wide array of physiologically active metabolites, thereby constituting an underutilized resource of natural products in plant system [8–13]. *Euphorbia* plants, widely used as folk medicines, have been shown to harbour a wealth of "privileged structures" with anti-fibrosis, anti-obesity, and anti-cancer potential in our prior research [14–17]. In the present study, we aimed to unveil the potential relationships between metabolites produced by *Euphorbia* plants and their associated endophytes. By analysing the secondary metabolites of *Euphorbia* endophytes using high performance liquid chromatography (HPLC) profiles and molecular networking [18], a strain named as *Malbranchea umbrina* D16 from the plant *Euphorbia wallichii* was highlighted from numerous members due to a protonated molecular ion cluster, within which a node (parent ion at *m*/*z* 491.374) was identified as a known tricyclic UCT, malbrancheogenin (**16**) (Fig. 1A) [19], implying that the fermentation extract of this endophyte might be a treasure-house of UCTs. As expected, subsequent large-scale fermentation and iso-

* Corresponding authors.
E-mail addresses: tanggh5@mail.sysu.edu.cn (G.-H. Tang), yinsh2@mail.sysu.edu.cn (S. Yin).
[1] These authors contributed equally to this work.

https://doi.org/10.1016/j.cclet.2025.111336
1001-8417/© 2026 Published by Elsevier B.V. on behalf of Chinese Chemical Society and Institute of Materia Medica, Chinese Academy of Medical Sciences.

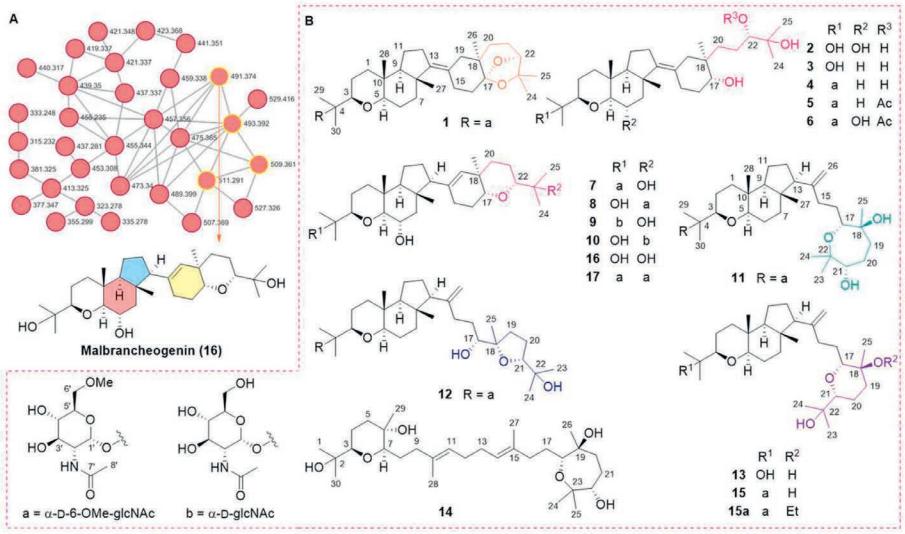


Fig. 1. (A) Clusters of nodes from *Malbranchea umbrina* D16 for unusually cyclized triterpenes. (B) Structures of **1**–**17** and **15a**.

lation characterized 14 new metabolites (Fig. 1B), including 10 tricyclic triterpenoids with 6/6/5–6 ring system differed in the appendage (6,8-dioxabicyclo[3.1.2]octane in **1**, acyclic chain in **2**–**6**, and oxane in **7**–**10**), three bicyclic triterpenoids containing a bicyclo[4.3.0]nonane core with an unusual long chain at C-13 (**11**–**13**), and one squalene derivative (**14**). Additionally, co-occurring triterpenes were obtained including malbrancheoside A (**15**), malbrancheogenin (**16**), and onygenaleoside F (**17**) (Fig. 1B) [19,20]. The discovery of **1**–**17** and **15a** provided the fertile ground with structurally diverse molecules for bioactivity screening. Notably, compound **1** was identified as a potent antiadipogenic agent, activating the AMP-activated protein kinase (AMPK) signalling to inhibit the adipogenesis in 3T3-L1 adipocytes. Herein, we disclose the isolation, structural elucidation, configurational revision, hypothetic biosynthetic pathways, and antiadipogenic evaluation of **1**–**17** and **15a**.

Malbrumpenoid A (**1**) was assigned a molecular formula of $C_{39}H_{63}NO_9$ with nine indices of hydrogen deficiency (IHD) from high resolution electrospray ionization mass spectroscopy (HRESIMS) ($[M+Na]^+$ *m*/*z* 712.4404, calcd. 712.4395). The existence of a α-6-*O*-methyl-*N*-acetylglucosamine (α-6-OMe-glcNAc) unit was indicated by typical signals of an anomeric proton at δ_H 5.19 (d, $J = 3.7$ Hz), a methoxy at δ_H 3.39, an acetyl group at δ_H 2.01, and a series of proton signals overlapped at δ_H 3.57–3.86, combined with the characteristic carbons signals at δ_C 172.1, 92.3, 74.7, 72.3 × 2, 70.0, 59.6, 54.4, and 23.5 (Table S1 in Supporting information) [21]. The remaining ^{1}H nuclear magnetic resonance (NMR) data (Table S1) displayed seven singlet methyls (δ_H 1.37, 1.24 × 2, 1.17, 0.99 × 2, 0.87), three oxymethines [δ_H 3.86 (m), 3.36 (brd, $J = 12.1$ Hz), and 3.01 (dd, $J = 11.7$, 2.5 Hz)], and a series of aliphatic methylene multiplets. Analysis of ^{13}C NMR and distortionless enhancement by polarization transfer (DEPT) spectra (Table S1) unveiled the remaining signals for a tetrasubstituted double bond (δ_C 142.7 and 124.5), a hemiketal carbon (δ_C 110.0), seven methyls, 11 sp^3 methylenes, four methines (three oxidized at δ_C 86.0, 85.3, and 81.5), two oxygenated sp^3 tertiary carbon (δ_C 79.8 and 79.6), and three quaternary carbons. Since the above functionalities occupied a total of three IHDs, thereby **1** was required to be equipped with hexacyclic fragments.

Interpretation of ^{1}H–^{1}H correlation spectroscopy (COSY) spectrum of **1**, five key spin systems, H_2-1/H_2-2/H-3, H-5/H_2-6/H_2-7, H-9/H_2-11/H_2-12, H_2-15/H_2-16, and H_2-20/H_2-21/H-22, were readily furnished by the corresponding cross-peaks. The assembly of these

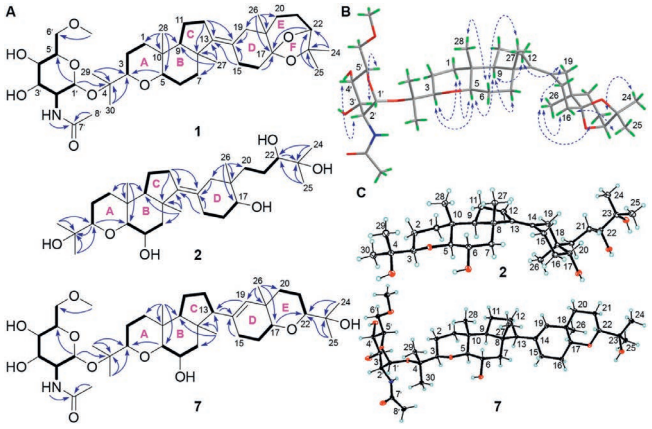


Fig. 2. (A) Key ^{1}H–^{1}H COSY (bold lines) and HMBC (solid arrows) correlations of **1**, **2**, and **7**. (B) Key NOESY (dashed arrows) correlations of **1**. (C) Oak ridge thermal ellipsoid plot (ORTEP) diagram of **2** and **7**.

units with hydrogen-free carbons and functionalities was achieved by detailed heteronuclear multiple bond correlation (HMBC) analysis (Fig. 2A). The HMBC correlations from H_3-28 to C-1, C-5, C-9, and C-10, from H-5 to C-3, from H_3-29 and H_3-30 to C-3 and C-4, from H_3-27 to C-7, C-8, C-9, and C-13, and from H_2-12 to C-8 and C-13 facilitated the fused A/B/C (6/6/5) tricyclic ring system. The glucosamine unit was located at C-4, by HMBC from H-1′ to C-4 (δ_C 79.6). The HMBC correlations from H_3-26 to C-17, C-18, C-19, and C-20, from H_2-15 and H_2-19 to C-14, and from H_2-16 and H-22 to C-17 established the 6/6-fused (D/E) ring system. In consideration of the remaining IHD and the unassigned oxygen atom in the molecule, an additional ring is still required in **1**. Thus, a *gem*–dimethyl-substituted 1,3-dioxolane moiety (F-ring) was proposed and confirmed by chemical shifts of C-17 (δ_C 110.0) and C-23 (δ_C 79.8) and HMBC associations from H_3-24 and H_3-25 to C-23. The above two tricyclic ring systems of A/B/C and D/E/F rings were readily connected through the tetrasubstituted bond Δ^{13} as supported by HMBC correlation of H_2-12/C-14 and H_2-15/C-13, thus constructing the 1-cyclohexyloctahydro-1*H*-indene carbon core fused with *O*-heterocycles in **1**. Hence, the gross structure of **1** with an unusual 7,7-dimethyl-6,8-dioxabicyclo[3.1.2]octane motif was delineated as depicted.

The relative configuration of **1** was assigned based on the analysis of nuclear Overhauser effect spectroscopy (NOESY) interactions (Fig. 2B) and coupling constants. As for the A/B/C rings, the NOE correlations of H-1α/H-3 and H-5, H-3/H-5, H-9/H-5 and H-7α, and H-6β/H_3-27 and H_3-28 indicated that these protons or functional groups were axially oriented on the chair-conformational six-membered A- and B-rings. Thus, H-3, H-5, and H-9 were arbitrarily assigned α-orientation, while CH_3-27 and CH_3-28 were β-configured. The NOE interaction of H-9/H-12α, H-12α/H-19α, and H_3-26/H-16α, H-19α, and H-21α required CH_3-26 to be axially α-oriented, while H-21β and H-16β showed correlations with H_3-24 (δ_H 1.37) and H_3-25 (δ_H 1.24), respectively, indicating that the C-22−C-23(CH_3-24/CH_3-25)−O−C-17 bridge extended above the E-ring. This hypothesis was further verified by the NMR calculation and DP4+ analysis on two possible isomers (17*S**,22*S** and 17*R**,22*R**). The final DP4+ score of 17*S**,22*S**−**1** (99.99 %) afforded an absolute advantage over that of the counterpart (Fig. S6 in Supporting information). Time-dependent density functional theory (TDDFT)-electronic circular dichroism (ECD) calculation for **1** and *ent*–**1** was further performed and compared with the experimental one, which allowed the absolute configuration of the aglycone to be explicitly assigned as 3*R*, 5*R*, 8*R*, 9*S*, 10*R*, 17*S*, 18*R*, 22*S* (Fig. S7 in Supporting information). To determine the absolute configuration of the sugar moiety, hydrolysis of **1** afforded the glycosyl moiety, which was determined as D-configuration by comparing its specific optical rotation value ([α] +42.50, *c* 0.50, MeOH) with literature values ([α] +50, *c* 0.10, MeOH) [21].

Malbrumpenoid B (**2**) was obtained as transparent blocky crystals with an elemental formula of $C_{30}H_{52}O_6$ by HRESIMS ($[M+Na]^+$ *m*/*z* 531.3648, calcd. 531.3656). Analysis of the NMR spectra (Table S2 in Supporting information) suggested the presence of a tetrasubstituted double bond (δ_C 143.2 and 126.5), seven methyls, ten sp^3 methylenes, six methines (five oxidized at δ_C 91.5, 87.0, 80.6, 75.7, and 68.4), two oxygenated sp^3 tertiary carbon (δ_C 73.9 and 73.6), and three quaternary carbons. The structure of **2** resembled those of aglycone of **1**, except that 1,3-dioxolane was cleaved to be a terminal 6-carbon acyclic segment (C-20–C-25) attached at C-18, which accounted for the upfield shifted chemical signals of C-17 (Δ34.3 ppm), C-22 (Δ0.9 ppm), and C-23 (Δ5.9 ppm) in **2**. The relative configuration of oxane-cycloalkane skeleton of **2** was assigned to be the same as **1** by NOESY analysis (Fig. S8 in Supporting information). Specially, the α-configuration of 17-OH was elucidated based on the NOE interaction between H-17 and H-19β, while the 22*S* configuration was determined by $Mo_2(OAc)_4$-induced ECD experiment [22], which displayed the positive Cotton effect at 310 nm (Fig. S9 in Supporting information). Finally, the X-ray crystallographic data explicitly proved the absolute configuration of **2** as 3*R*, 5*S*, 6*S*, 8*R*, 9*S*, 10*R*, 17*R*, 18*R*, 22*S* (Fig. 2C).

Analysis of the ^{13}C NMR data of malbrumpenoids C-F (**3**–**6**) (Tables S1 and S2) showed the presence of a pair of tetrasubstituted double bond signals, indicating that they belong to the same compound class as **2**, with the major structural difference being the oxidation pattern at C-6 and substitution at C-4 or C-22. Compound **3** was verified to lack a 6-OH group by ^1H–^1H COSY correlation of H-5/H_2-6 (Fig. S10 in Supporting information), while **4**–**6** were determined to be triterpene glycosides containing a α-D-6-OMe-glcNAc at C-4 as inferred from the spectroscopic analysis and positive optical rotation of released sugar moiety [21]. Further interpretation of their 2D NMR and MS data suggested that **4** and **5** shared a similar aglycone part to **3** (**5** was a 22-acetylated derivative of **4**) (Fig. S10), while the aglycone of **6** was a 22-acetoxylated analogue of **2**. The stereochemistry of **3**–**6** was assigned to be identical with that of **2** by comparing their NMR, NOESY, and ECD data (Fig. S11 in Supporting information).

Malbrumpenoids G and H (**7** and **8**) were established to be monosaccharide derivatives of malbrancheogenin (**16**) by NMR (Table S3 in Supporting information) and MS data [19,21]. Their sugar moiety was determined to be α-6-OMe-glcNAc by comparison of the chemical shifts with those of **1**. Their position was determined to be at C-4 in **7** and at C-23 in **8** by HMBC analysis, respectively (Fig. 2A). Similarly, malbrumpenoids I and J (**9** and **10**) were assigned as another pair of triterpene glycosides, with the major difference being that their sugar moieties were replaced by a α-*N*-acetylglucosamine (α-glcNAc) moiety in **9** and **10** (Fig S10). Combined with X-ray diffraction analysis of **7** (Fig. 2C) and hydrolysis of **7**−**10** and **17** to **16**, the stereochemistry of **8**−**10**, **16**, and **17** is consistent with that of **7**. The D-configuration of glucosyl moiety in **7**–**10** and **17** was determined by positive specific optical rotation values of the released sugar [21]. The potential atropisomerism of compounds **7**–**10**, **16**, and **17** arising from the hindered rotation of C-13–C-14 bond was addressed through NOESY cross-peaks between H-19 and H-12β in their common aglycone part (**16**) (Fig. S8) as well as single-crystal X-ray diffraction analysis of **7**, which confirmed a single dominant atropisomeric form in both solution and solid state, consistent with the depicted stereochemistry.

Malbrumpenoid K (**11**) had a molecular formula of $C_{39}H_{67}NO_{10}$ based on a protonated adduct peak at *m*/*z* 710.4833 $[M+H]^+$ (calcd. 710.4838) in the HRESIMS. Scrutiny of the NMR data of **11** (Table S4 in Supporting information) indicated a tetracyclic triterpene glycoside reminiscent of onygenaleoside F (**15**) [20], with the main structural difference being the oxygen heterocyclic D-ring. The HMBC correlation of H-17/C-22 undoubtedly demonstrated a 17,22-ether linkage, furnishing a D-ring as an oxepane in **11** instead of an oxane in **15** (Fig. 3A). The relative configuration of the tricyclic moiety (A/B/C rings) in **11** was assigned to be the same as **7** based on their comparable NOESY analysis. Specially, the NOE correlation of H-9/H-13 revealed that H-13 was α-oriented. As for the D-ring, the NOE correlations of H_3-23/H-17 and H-21 showed both H-17 and H-21 were β-configured, while the interactions of H-20α/H_3-24 and H_3-25 revealed an α-orientation for CH_3-25 (Fig. 3B).

Malbrumpenoid L (**12**) shared the same molecular formula of $C_{39}H_{67}NO_{10}$ as **11** and **15**, implying that **12** was an isomer of **11** and **15** [20]. Analysis of their similar NMR data suggested that the major difference among these compounds lied in the cyclization position of the ether ring (D-ring). In particular, the downfield-shifted C-18 ($\Delta\delta_C$ 11.5) and C-21 ($\Delta\delta_C$ 8.0) signals with respect to those in **11** (Table S4) indicated an oxygen bridge between C-18 and C-21 to construct a pentacyclic D-ring. Although no HMBC correlations were observed to support the hypothesis, isotope shift experiments measured in CD_3OD and CD_3OH confirmed that C-18 (δ_C 86.7) and C-21 (δ_C 88.1) with no obvious deuterium-induced isotope shift should be involved in the ether linkage (Fig. S115 in Supporting information) [23]. The 17*R*-configuration in the side chain was determined by means of Mosher's method (Fig. 3C) [24]. Although the side chain might rotate around the bond C-17–C-18 in solution, the strong NOE interaction of H-17/H-19β and H_3-25/H-19α implied the existence of a stable conformation in which the H-17 and CH_3-25 adopted β- and α-orientations, respectively (17*R*, 18*R*) (Fig. 3B). Combined with the interaction of H-19β/H-21 (21*R*), the stereochemistry of **12** was assigned as depicted.

Malbrumpenoid M (**13**) was assigned an elemental formula of $C_{30}H_{52}O_5$ by HRESIMS ($[M+Na]^+$ *m*/*z* 515.3732, calcd. 515.3707). Interpretation of NMR data of **13** and **15** revealed that the characteristic signals for sugar moiety were absent in **13** [20], indicating that **13** was the aglycone of **15**. This hypothesis was verified by the noticeable upfield shifted carbon signal at C-4 (δ_H 72.1 in **13**; δ_H 79.4 in **15**) (Table S5 in Supporting information). Particularly, the NOE correlations of H-19β/H-17 and H-21 and H-20α/H_3-25 indicated that these protons or functional groups were axially ori-

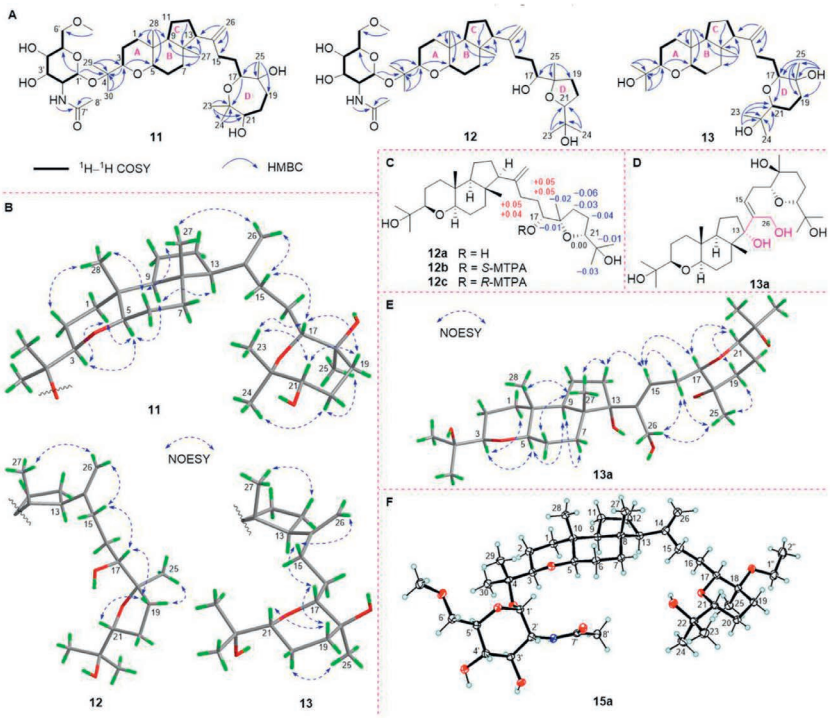


Fig. 3. (A) Key ^{1}H–^{1}H COSY and HMBC correlations of **11**–**13**. (B) Key NOESY correlations of **11**–**13**. (C) $\Delta\delta^{SR}$ values obtained for **12a**. (D) Structure of **13a**. (E) Key NOESY correlations of **13a**. (F) ORTEP diagram of **15a** at 25% ellipsoid probability.

ented on the chair-conformational six-membered D-ring. Thus, H-17 and H-21 were β-oriented, while CH_3-25 was assigned an α-orientation (Fig. 3B).

However, NOESY interactions were not persuasive to determine the relative configuration between the two separate ring systems in **11**–**13** due to the large interatomic spacing conferred by the branched 3- or 4-carbon chain. Thus, we resorted to Shibuya allylic oxidation of **13** [25], which unexpectedly generated a dihydroxyl derivative **13a** (Fig. 3D). Further NOESY analysis showed that H-15 correlated with H-16β, H-17, and H-12β; simultaneously, H-16α showed correlations with H_3-25 and H_2-26, which helped complete the stereochemical assignment as depicted (Fig. 3E). Finally, the X-ray crystallographic result of 18-ethoxy-onygenaleoside F (**15a**, which is a possible artifact of isolation) allowed the unequivocal assignment of the absolute configuration of these tetracyclic triterpenes (Fig. 3F). Given the compatible ECD curves of **15** and **15a** (Fig. S11 in Supporting information), the stereochemistry of **15** was thus correlated with that of **15a**. Since the ordinary acid hydrolysis of **15** in concentrated HCl or H_2SO_4 would result in the degradation of the aglycone, **15** was subjected to the hydrolysis under a mild condition, *i.e.* Smith's degradation [26], which fortunately generated the genuine aglycone **13**. The D-configuration of α-6-OMe-glcNAc in **11**, **12**, and **15a** was inferred by the positive specific optical rotation values of the released sugar [21].

Malbrumpenoid N (**14**) was assigned a molecular formula of $C_{30}H_{54}O_6$ by HRESIMS ($[M+Na]^+$ *m/z* 533.3837, calcd. 533.3813) with four IHDs. While the NMR pattern of **14** (Table S2) was similar to that of the aglycone of **11** (Figs. S182 and S183 in Supporting information), two typical sp^3 methines occurring at around δ_C 59 (C-9 and C-13 in **11**) was absent in **14**, implying that **14** is an acyclic oxidosqualene derivative. The planar structure of **14** was further deduced by inspection of 2D NMR spectra (Fig. 4A). According to ^{1}H-^{1}H COSY cross-peaks, six spin systems, H-3/H_2-4/H_2-5, H-7/H_2-8/H_2-9, H-11/H_2-12, H_2-13/H-14, H_2-16/H_2-17/H-18, and H_2-20/H_2-21/H-22, were observed. The HMBC correlations from H-3 to C-7, from H_3-29 to C-5, C-6, and C-7, and from H_3-1 and H_3-30 to C-2

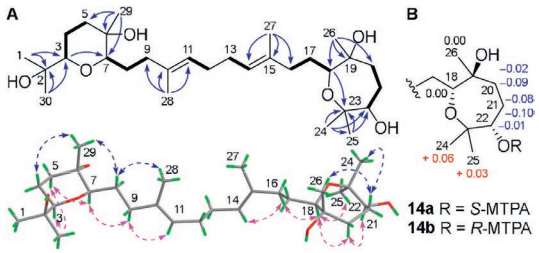
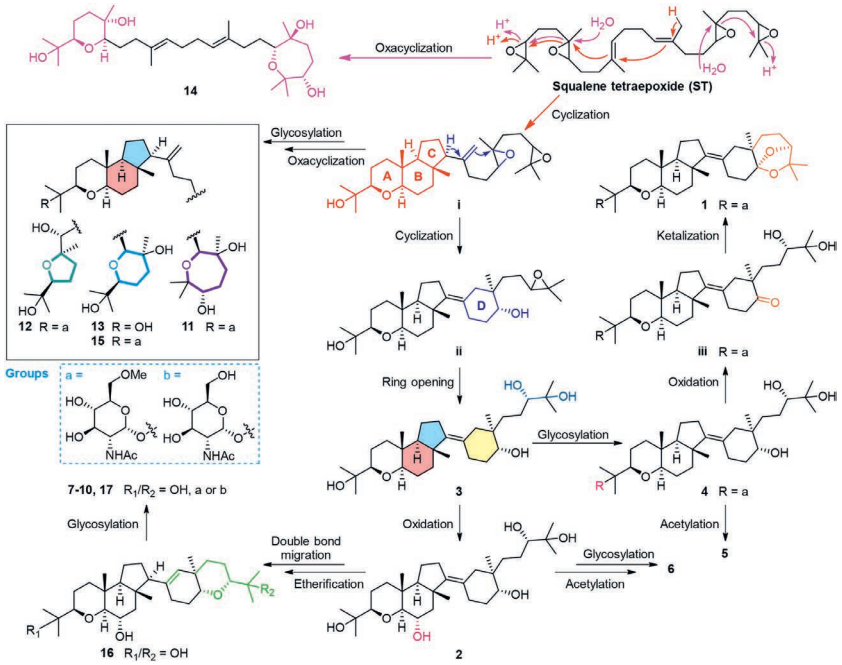


Fig. 4. (A) Key ^{1}H–^{1}H COSY (bold lines), HMBC (solid arrows), and NOESY (dashed arrows) correlations of **14**. (B) $\Delta\delta^{SR}$ values obtained for **14**.

and C-3 facilitated a tetrahydropyran, which was connected with a heterocyclic ring through a branched 10-carbon acyclic segment as verified by HMBC analysis combined with MS data. The relative configuration of **14** was determined by NOESY analysis (Fig. 4A). The NOE interactions of H-5α/H-3 and H-7 as well as H-4β/H_3-29 suggested that H-3 and H-7 were axially α-configured and CH_3-29 was axially β-oriented, while the correlations of H-8b/H_3-28, H-9a/H-11, and H-16a/H-14 assigned the geometry of Δ^{10} and Δ^{14} as *E*. Similarly, the relative configuration of oxepane was assigned to be identical to that in **11** based on their similar NOESY analysis. The absolute configuration of C-22 was determined to be *S* by Mosher analysis (Fig. 4B) [24]. Given the biosynthetic consideration, the stereochemistry of **14** was depicted as shown.

The hypothetical biogenetic pathway of compounds **1**–**17** has been proposed to involve two distinct cyclization processes of squalene tetraepoxide (ST) (Scheme 1). The truncated cyclization of the left half in ST initially generated intermediate **i** with a fused tricyclic moiety (A/B/C rings). Then, the abstraction of H-13 in **i** triggered the cyclization on its right half to form intermediate **ii** with an additional D-ring. Subsequent ring opening and oxidation of **ii** yielded **3** and **2**, with the latter progressing to **16** *via* etherification and double-bond isomerization. Scaffold decoration of **3** and **16** through glycosylation, acetylation and/or oxidation gave



Scheme 1. Plausible biosynthetic pathways for **1**–**14**.

rise to the structures of **4**–**10** and **17**. Notably, compound **4** served as a key precursor, undergoing oxidation at C-17 to access **iii**, followed by intramolecular ketalization to construct a 7,7-dimethyl-6,8-dioxabicyclo[3.1.2]octane motif in **1**. In a parallel pathway, the oxacyclization of the remaining diepoxide in **i** through regioselective epoxide opening, followed by glycosylation, completed the biosynthesis of **11**–**13** and **15**. From a bypass, a dual oxacyclization of epoxides in ST led to the formation of **14**.

The triglyceride (TG)-lowering activity of compounds **1**–**17** and **15a** was evaluated in a 3T3-L1 adipocytes model, with metformin (Glucophage, 10 mmol/L) as the positive drug (Fig. 5A) [27]. Among them, **1** dose-dependently decreased the TG level from 1 μmol/L to 20 μmol/L as verified by Oil Red O (ORO) staining experiments, with an median effective concentration (EC_{50}) value of 9.26 ± 1.02 μmol/L (Figs. 5B and C).

AMPK is implicated in regulating the lipid metabolism. Activation of AMPK in 3T3-L1 cells inhibited the expression of downstream transcriptional factors and fatty acid synthesis-related proteins, thus suppressing adipogenesis [28,29]. As shown in Fig. 5D, treatment with **1** significantly increased the activated AMPK (p-AMPK) in a dose-dependent manner, indicating AMPK activation. Consistently, the expression of key transcriptional factors, peroxisome proliferator activated receptor γ (PPARγ) and CCAAT-enhancer-binding protein α (C/EBPα), were significantly decreased, accompanied by the down-regulation of downstream lipogenic proteins such as fatty acid synthase (FAS), acetyl CoA carboxylase (ACC), and stearoyl-CoA desaturase-1 (SCD1). Altogether, these results suggested that **1** inhibited adipogenesis in 3T3-L1 cells by activating AMPK signalling.

Stereochemical difference could arise within the same class of compounds depending on their terrestrial or marine origins. A notable case is the peribysin family, among which peribysin Q from the plant exhibits the opposite absolute stereochemistry to the marine counterpart, as confirmed by enantiospecific total synthesis [30]. In this study, 14 novel UCTs were isolated from the *Euphorbia* endophyte *M. umbrina* D16. Intriguingly, compounds **1**–**14**, **15a**, and previously reported analogues displayed opposite sign of rotation to that of marine-derived abudinol B ($[\alpha]_D$ −5) [19,20,31,32], implying UCTs derived from terrestrial fungi may employ distinct cyclization mechanism compared to their marine counterparts. To address such issue, X-ray diffraction technique was employed to corroborate the stereochemistry of **1**–**14** and **15a** as opposite to that of abudinols, and to facilitate the reassignment of the co-isolated analogues as **15**–**17**. Accordingly, the aglycone of

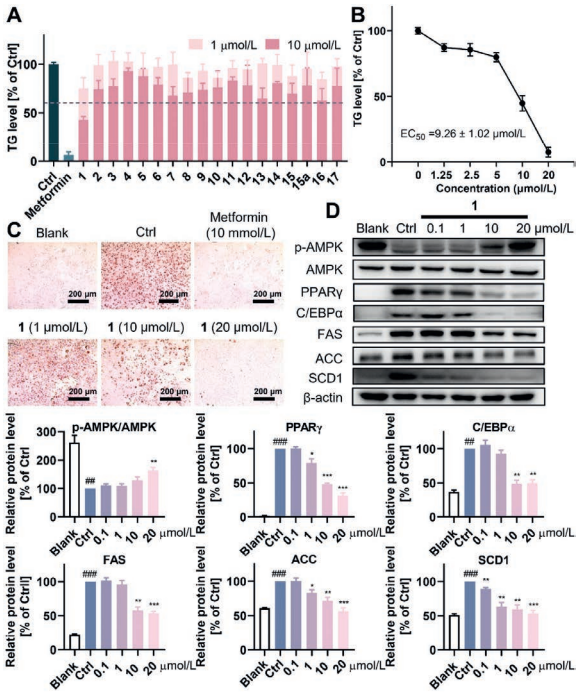


Fig. 5. (A) Effects of indicated compounds (1 or 10 μmol/L) on the TG level in 3T3-L1. (B, C) Dose-dependent effect of **1** on the TG level in 3T3-L1. (D) Effect of **1** on the expression of AMPK, p-AMPK, indicated differentiation factors, and fatty acid synthesis-related proteins at different concentrations in 3T3-L1: blank, undifferentiated cells; Ctrl, differentiated cells without compound treatment. Data represent the mean ± the standard deviation of at least three independent experiments. $^{\#\#}P < 0.01$, $^{\#\#\#}P < 0.001$ *vs.* the blank group; $^{*}P < 0.05$, $^{**}P < 0.01$, $^{***}P < 0.001$ *vs.* the control group.

previously reported malbrancheosides and onygenaleosides require stereochemical revision as the corresponding enantiomers [19,20].

In conclusion, the discovery of **1**–**14** and **15a** offers new insights into the oxacyclization processes of oxidosqualene, affording diverse chemical entities within the class of UCT. Unlike soil fungi-derived analogues, which typically feature an oxane on the right half of the structure [19,20], compounds identified in this study contain more modified appendages (6,8-dioxabicyclo[3.1.2]octane in **1**, 6-carbon acyclic segment in **2**–**6**, oxepane in **11** and **14**, and oxolane in **12**). Such structural diversity highlights the pivotal role of host plants in shaping the metabolic profiles of associated endophytes. From a biological perspective, **1** displayed potent antiadipogenic efficacy at 10 μmol/L. Compared to other UCTs, the newly introduced 1,3-dioxolane motif appears to rendered **1** enhanced activity, which provides a privileged scaffold for future anti-obesity drug development.

Declaration of competing interest

The authors declare that they have no known competing financial interests or personal relationships that could have appeared to influence the work reported in this paper.

CRediT authorship contribution statement

Shu-Qi Wu: Writing – original draft, Validation, Methodology, Investigation, Data curation. **Xinying Zhu:** Methodology, Investigation, Data curation. **Fang-Yu Yuan:** Writing – review & editing, Funding acquisition. **Han-Zhuang Weng:** Methodology, Investigation. **Lei Li:** Data curation. **Dong Huang:** Writing – review & editing, Funding acquisition. **Gui-Hua Tang:** Writing – review & editing, Supervision, Project administration, Conceptualization. **Sheng Yin:** Writing – review & editing, Supervision, Funding acquisition, Conceptualization.

Acknowledgments

This work was supported by the National Natural Science Foundation of China (Nos. 81973195, 82273804, 22407144, and 82404454), the Science and Technology Program of Guangzhou, China (No. 2024B03J1322), the Science and Technology Planning Project of Guangdong Province, China (No. 2023A1111120025), the Postdoctoral Fellowship Program of CPSF (No. GZC20242113), and the China Postdoctoral Science Foundation (No. 2024M753800).

Supplementary materials

Supplementary material associated with this article can be found, in the online version, at doi:10.1016/j.cclet.2025.111336.

References

[1] Z.R. Goddard, M. Searcey, A. Osbourn, Trends Pharmacol. Sci. 45 (2024) 964–968.
[2] V. Domingo, J.F. Arteaga, J.F. Quílez del Morala, et al., Nat. Prod. Rep. 26 (2009) 115–134.
[3] H. Hussain, J. Xiao, A. Ali, et al., Nat. Prod. Rep. 40 (2023) 412–451.
[4] Q. Xiong, W.K. Wilson, S.P. Matsuda, Angew. Chem. Int. Ed. 45 (2006) 1285–1288.
[5] F.E. McDonald, R. Tong, M.A. Boone, et al., Strateg. Tactics Org. Synth. 8 (2012) 225–260.
[6] S. Peng, Y. Guo, M. Irondelle, et al., Cell Mol. Biol. Lett. 29 (2024) 101.
[7] R.X. Tan, W.X. Zou, Nat. Prod. Rep. 18 (2001) 448–459.
[8] S. Waqar, A.A. Bhat, A.A. Khan, Plant Physiol. Biochem. 206 (2024) 108174.
[9] G.P. Yin, Y.J. Li, L. Zhang, et al., Chin. Chem. Lett. 35 (2024) 109035.
[10] A. Fu, C. Chen, Q. Li, et al., Chin. Chem. Lett. 35 (2024) 109100.
[11] Q. Tan, R.Z. Fan, W. Yang, et al., Chin. Chem. Lett. 35 (2024) 109390.
[12] H. Zhang, C.P. Li, L.L. Wang, et al., Chin. Chem. Lett. 35 (2024) 109351.
[13] L. Li, X.Y. Zhu, J.Y. Zhu, et al., Chin. Chem. Lett. 37 (2026) 111161.
[14] Z.J. Zhan, S. Li, W. Chu, et al., Nat. Prod. Rep. 39 (2022) 2132–2174.
[15] L. Gan, Q. Jiang, D. Huang, et al., Nat. Chem. Biol. 21 (2025) 80–90.
[16] J.L. Huang, X.L. Yan, W. Li, et al., J. Am. Chem. Soc. 144 (2022) 17522–17532.
[17] X.L. Yan, Y.H. Pan, R.Z. Fan, et al., J. Med. Chem. 66 (2023) 5839–5858.
[18] M. Wang, J.J. Carver, V.V. Phelan, et al., Nat. Biotechnol. 34 (2016) 828–837.
[19] D. Wakana, T. hosoe, T. Itabashi, et al., Heterocycles 75 (2008) 1109–1122.
[20] K. Chen, J. Zhou, B. Dun, et al., J. Nat. Prod. 86 (2023) 2621–2629.
[21] A.A. Dewa, Z.G. Khalil, W.M. Hussein, et al., J. Nat. Prod. 87 (2024) 935–947.
[22] L. Di Bari, G. Pescitelli, C. Pratelli, et al., J. Org. Chem. 66 (2001) 4819–4825.
[23] Y. Hamamoto, K. Tachibana, P.T. Holland, et al., J. Am. Chem. Soc. 134 (2012) 4963–4968.
[24] I. Ohtani, T. Kusumi, Y. Kashman, et al., J. Am. Chem. Soc. 113 (1991) 4092–4096.
[25] K. Shibuya, Synth. Commun. 24 (1994) 2923–2941.
[26] M. Nagai, T. Ando, N. Tanaka, et al., Chem. Pharm. Bull. 20 (1972) 1212–1216.
[27] L. Ma, C. Xie, Y. Ran, et al., J. Med. Chem. 55 (2012) 9958–9972.
[28] D. Garcia, R.J. Shaw, Mol. Cell 66 (2017) 789–800.
[29] J. Massagué, Nat. Rev. Mol. Cell Biol. 13 (2012) 616–630.
[30] P.R. Athawale, H.P. Kalmode, Z. Motiwala, et al., Org. Lett. 22 (2020) 3104–3109.
[31] A. Rudi, T. Yosief, M. Schleyer, et al., Tetrahedron 55 (1999) 5555–5566.
[32] R. Tong, J.C. Valentine, F.E. McDonald, et al., J. Am. Chem. Soc. 129 (2007) 1050–1051.